Available online at www.sciencedirect.com
SCIENCE DIRECT
Polymer 47 (2006) 4218–4229
polymer
www.elsevier.com/locate/polymer

Dielectric relaxation behavior of poly(acrylonitrile-*co*-methacrylonitrile) microcapsules dispersed in a silicone matrix

Taigyoo Park [a], Emmett O'Brien [a], Jeremy R. Lizotte [a], Thomas E. Glass [a], Thomas C. Ward [a,*], Timothy E. Long [a], Donald J. Leo [b]

[a] *Department of Chemistry, Virginia Polytechnic Institute and State University, Blacksburg, VA 24061, USA*
[b] *Mechanical Engineering, Virginia Polytechnic Institute and State University, Blacksburg, VA 24061, USA*

Available online 18 April 2006

Abstract

The dielectric relaxation behavior of poly(acrylonitrile-*co*-methacrylonitrile) dispersed in a cured polydimethyl siloxane (PDMS) matrix as microcapsules was investigated over multiple thermal cycles and at varying concentrations. The copolymer microcapsules contained an isopentane core. In the PDMS matrix this copolymer displayed a pronounced relaxation signal at temperatures above the glass transition of the copolymers due to Maxwell–Wagner–Sillars (MWS) relaxation. The mechanism of MWS relaxation interpreted by the Havriliak–Negami and Kohlrausch–Williams–Watts relaxation functions was found to be very similar to previous studies of neat polyacrylonitrile and its copolymer. The activation energy of the relaxation decreased over successive thermal cycling coincident with a decreasing strength of the relaxation. These observations were attributed to the decreasing concentration of nitrile groups due to intramolecular cyclizations.

Keywords: Dielectric relaxation behavior; Polyacrylonitrile; Copolymer

1. Introduction

The relaxation behavior of polyacrylonitrile (PAN) copolymers has been studied extensively due to the commercial importance of acrylonitrile containing copolymers, which are used as raw materials for fibers and as a precursor in carbon fiber production. Other examples of studies on the relaxation behavior of PAN copolymers include those with 1,3-butadiene for rubber applications [1], methyl vinyl ether for fibers [2], and styrene for engineering thermoplastics [3]. Recent interest in a PAN block copolymer of *n*-butyl acrylate includes a potential application in the fabrication of nanostructured carbon arrays after pyrolysis of the acrylate phase [4]. Historically, an understanding of the relaxation behavior of PAN and its copolymers on a molecular level often has been incomplete and sometimes controversial [5]. It is now well established that PAN and its copolymers (with acrylonitrile as a major component) undergo intramolecular cyclization of the pendant nitrile groups at temperatures as low as 160 °C under vacuum [6]. The usual sample preparation method for dielectric or dynamic mechanical analysis involves solution casting of a film using a high boiling point solvent such as dimethyl formamide (DMF). It is not surprising that thermal aging processes, as well as temperature and atmosphere exposures associated with the film drying procedure, could affect the dielectric experimental results of PAN homopolymers and copolymers in previous studies. We anticipate an increasing direct current (Dc) conductivity in these polymers at high-temperature due to the cyclization of pendant nitrile groups considering that the fully cyclized PAN (carbon fiber) is conductive.

In this study, the relaxation behavior of a PAN copolymer with methacrylonitrile was investigated by forming it into the walls of microcapsules containing an isopentane core, which were dispersed in a polydimethyl siloxane (PDMS) matrix. This experimental approach was chosen primarily to avoid a solution casting process, which potentially introduces thermal aging during the production of well-dried thin films. Another positive feature of our sample is that the materials may not exhibit significant dc conductivity during dielectric study as the PAN turns into an inherently more conductive material during the thermal scanning. This significant advantage could be expected given the nonpercolating nature of the encapsulated polymer, which thus offers no direct conductive pathway between the capacitor plates. However, our approach also introduces more interfaces to the system. Interfaces between

* Corresponding author. Tel.: +1 540 231 5867; fax: +1 540 231 3255.
E-mail address: tward@vt.edu (T.C. Ward).

0032-3861/$ - see front matter © 2006 Elsevier Ltd. All rights reserved.
doi:10.1016/j.polymer.2006.03.056

the matrix and the copolymer shell (PDMS/PAN copolymer) and that between the copolymer shell and core (PAN copolymer/isopentane) are generally thought to lead to interfacial polarizations under electric fields due to a build-up of charge at the interfaces. Interfacial polarization has been observed extensively in heterogeneous systems including dispersions of a glass-beads in polystyrene [7], carbon black in poly(vinyl chloride) [8], liquid crystalline polymer fibers in polypropylene [9], and poly(ethylene oxide) inclusions in polycarbonate [10]. Interfacial polarization of a polystyrene microcapsule, which contains water in the core was studied as early as 1983 by Zhang et al. [11]. Mathematical modeling of interfacial polarization phenomena due to Maxwell, Wagner, and Sillars (MWS) has been extended by several workers and summarized in a recent review by Asami [12].

While there have been quite a few examples of the use of interfacial polarization in studying polymer miscibility, or of the shape factor of dispersed phases, not many cases have been reported concerning MWS polarization in order to understand the relaxation mechanism of the dispersed phases upon thermal aging. In this work, we attempted to observe the relaxation behavior of a dispersed phase (PAN copolymer) undergoing a thermal aging by using the MWS relaxation of the total microcapsule composite system. In the following, Eq. (1) expresses the complex permittivity of a suspension of spherical particles and Eq. (2) describes complex permittivity of the particles composed of a shell and core [12]

$$\frac{\varepsilon^*(\omega)-\varepsilon_m^*(\omega)}{\varepsilon^*(\omega)+2\varepsilon_m^*(\omega)}=\phi\frac{\varepsilon^*(\omega)-\varepsilon_p^*(\omega)}{\varepsilon^*(\omega)+2\varepsilon_p^*(\omega)} \tag{1}$$

where the complex permittivity of the system, $\varepsilon^*(\omega)$, is expressed with contributions from the matrix (suffix m) and the particles (suffix p) and ϕ represents the volume fraction of the particles in the suspension and

$$\varepsilon_p^*(\omega)=\varepsilon_s^*(\omega)\frac{2(1-\nu)\varepsilon_s^*(\omega)+(1+2\nu)\varepsilon_c^*(\omega)}{(2+\nu)\varepsilon_s^*(\omega)+(1-\nu)\varepsilon_c^*(\omega)} \tag{2}$$

where the complex permittivity of the microcapsule is expressed with contributions from the core (suffix c) and the shell (suffix s) and ν is a dimensionless parameter related to the volume fraction of the core phase in the microcapsule.

It should be noted that Eq. (1) dictates that the observed dielectric dispersion behavior $\varepsilon^*(\omega)$ reduces to that of the matrix $\varepsilon_m^*(\omega)$ when the particles are not present ($\phi=0$), or is related to $\varepsilon_p^*(\omega)$ by a constant factor (that is a function of ϕ) when the contribution from the matrix is negligible. Likewise, the complex permittivity of the microcapsule $\varepsilon_p^*(\omega)$ becomes proportional to the shell $\varepsilon_s^*(\omega)$ by a constant factor (as a function of ν) when the contribution from the core is negligible. Several assumptions (such as ignoring distribution in the wall thickness and size of microcapsules, perfect sphericity and the relatively dilute particle concentration, among others) have been made in arriving at Eqs. (1) and (2). These models, provided that the matrix and core materials are carefully selected to comply within an experimental temperature range and test frequencies, will be exploited in investigating the intrinsic properties of the shell materials, $\varepsilon_s^*(\omega)$, from the observed MWS relaxation behavior $\varepsilon^*(\omega)$. Thermogravimetric analysis (TGA) was also utilized to aid in the understanding of the diffusion processes of isopentane through the PAN copolymer shell. The dielectric relaxation spectra were interpreted in terms of the Havriliak–Negami and Kohlrausch–Williams–Watts relaxation function as proposed earlier by Alvarez et al. [13].

2. Experimental

Dielectric measurements were performed in the frequency range of 10^2–10^5 Hz over a temperature range of 30–200 °C with a DEA 2970 dielectric analyzer (TA Instruments®). During the dielectric experiments, normal stress on the gold plated electrodes was controlled at 87 kN/m^2 under a nitrogen atmosphere. Thermal cycling was accomplished by heating and cooling the samples at 1 °C/min while capacitance signals are acquisitioned by frequency sweeps. TGA was performed on a TGA 2950 Hi-Res Thermogravimetric analyzer (TA Instruments®). All samples were analyzed under a nitrogen atmosphere. Multiple heating rates of 5, 10, 20, and 40 °C/min were used for activation energy analysis.

The PAN copolymer microcapsule (Micropearl® F100D) was obtained from Sovereign Specialty Chemicals. Average spherical particle sizes ranged from 20 to 30 μm with shell thickness varying from 1 to 4 μm were obtained using scanning electron microscopy [14]. The chemical composition of the microcapsule was analyzed in dimethyl-d_6 sulfoxide (DMSO-d_6) using ^{1}H and ^{13}C nuclear magnetic resonance (NMR) spectroscopy utilizing a Varian Unity 400 MHz spectrometer. ^{1}H NMR spectra were acquired at 400 MHz over 128 scans with a 57° pulse. The acquisition time and relaxation delay were 3.7 and 1 s, respectively. ^{13}C NMR spectra were acquired at 100 MHz with continuous proton decoupling over 4800 scans with a 45° pulse. The acquisition time and relaxation delay were 1.2 and 1 s, respectively.

PDMS (Sylgard® 182) was obtained from Dow Corning Corporation. In order to prepare thin films with finely dispersed microcapsules, a PDMS solution was prepared as described earlier [15]. Subsequently, PAN copolymer microcapsules were added to the PDMS solution at 5, 10, 20, 30, and 35 parts per hundred (phr) (approximately 4.8, 9.1, 17, 23, and 26% by weight, respectively), followed by gentle stirring with a spatula. The mixture was finally cast on Teflon® plate and doctor-bladed using a 110 μm clearance. Curing of the PDMS composite was performed for 12 h at 100 °C. Films were obtained with thickness in the range of 90–105 μm, and were stored in desiccators prior to the dielectric measurements.

3. Results and discussion

3.1. NMR and TGA

^{1}H and ^{13}C NMR spectra of the PAN copolymer microcapsule are shown in Fig. 1. ^{13}C resonances for isopentane were sharp and without fine structure. Methylene

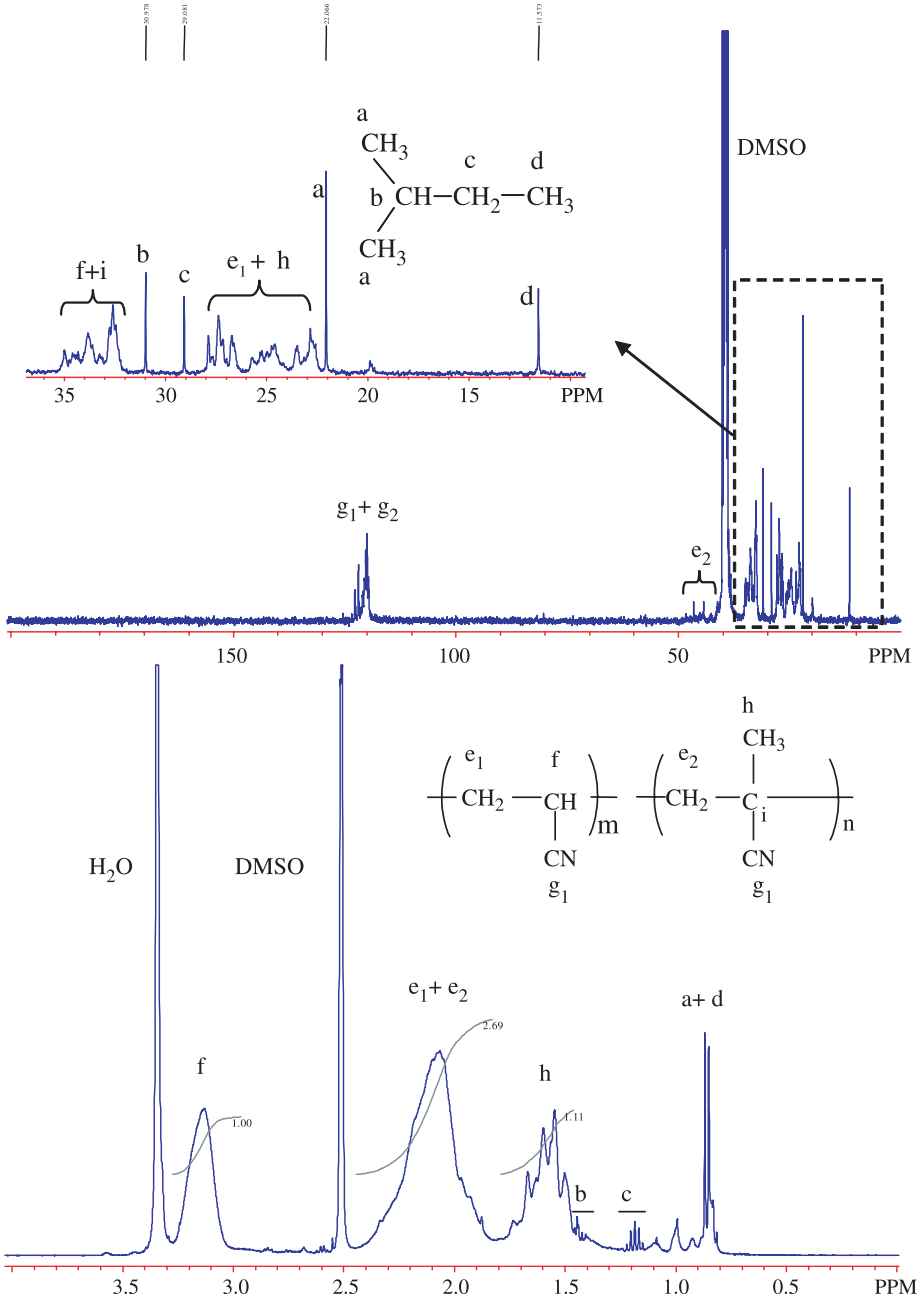

Fig. 1. ^{1}H and ^{13}C NMR spectra of the PAN copolymer microcapsule: (top) ^{13}C NMR; (bottom) ^{1}H NMR spectrum.

(δ 29.08), methyne (δ 30.98), methyl adjacent to methylene (δ 11.57), and methyl adjacent to methyne (δ 22.07) groups in isopentane were enlarged for clarity. Methyne ($\delta\sim25$) and methylene ($\delta\sim34$) carbons in poly(acrylonitrile) appeared as multiplets due to tacticity as reported previously [16]. The methylene ($\delta\sim48$) and quarternary ($\delta\sim33$) carbons of poly(methacrylonitrile) also displayed tacticity [17]. Based on the ratio of the methylene protons of both polyacrylonitrile (e_1) and poly(methacrylonitrile) (e_2) to the methyne protons of polyacrylonitrile (f), the poly(methacrylonitrile) content in the PAN copolymer was estimated to be 27 mol%.

TGA curves for the PAN copolymer microcapsules, the PDMS control, and the PAN copolymer microcapsules (35 phr) in PDMS (abbreviated as Film-A in the following) are shown in Fig. 2. Within the temperature range of interest (30–200 °C), PDMS exhibited no weight loss. However, the microcapsule lost approximately 15% by weight between 150 and 250 °C. The TGA curve of Film-A reflected the thermal degradation steps of both the microcapsules and the PDMS. Previously Xue et al. documented TGA curves of several polyacrylonitriles including commercial samples and reported no weight loss until 250 °C [6]. Moreover, according to Grassie and McNeill, who studied the thermal degradation of polyacrylonitrile and related polymers including poly(methacrylonitrile), weight loss below 200 °C was not observed (Fig. 1 in Ref. [18]). Therefore, the weight loss exhibited by our microcapsule was

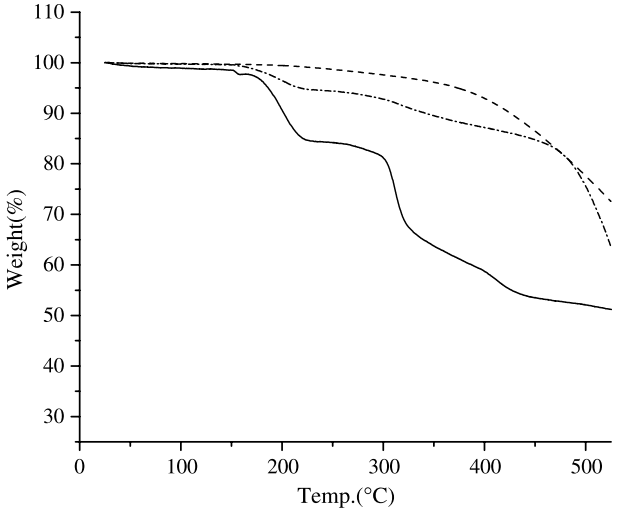

Fig. 2. TGA curves of PAN copolymer microcapsule (solid line), PDMS (broken line), and PAN copolymer microcapsule (35 phr) in PDMS (dashed line) (5 °C/min heating rate under nitrogen atmosphere).

attributed to the loss of isopentane, which diffused through the PAN copolymer shell. The onset temperature of weight loss (140 °C) occurred above the glass transition temperatures of both polyacrylonitrile (80–105 °C) [19] and poly(methacrylonitrile) (67–120 °C) [20] homopolymers, which further supports liberation of isopentane from the microcapsule core. In order to verify the time scale of the diffusion of isopentane through the PAN copolymer shell and the PDMS matrix, TGA was performed in a cyclic manner for both the microcapsule and Film-A and compared with single heat TGA curves as shown in Fig. 3. The diffusion of isopentane was nearly completed for both the microcapsule and Film-A during the first heat. In Fig. 4, TGA curves of Film-A at various heating rates are shown with plots of logarithmic heating rate versus reciprocal absolute temperature in order to evaluate the activation energy for the weight loss process due to the diffusion of isopentane through both the PAN copolymer shell and PDMS matrix. The activation energies for selected levels of conversion were evaluated using $E \cong -(R/0.457)d \log B/d(1/T)$ where B is the heating rate according to the method of Flynn [21]. The activation energies for the microcapsule and Film-A were 121 ± 4 and 131 ± 14 kJ/mol, respectively. The higher activation energy for the Film-A is thought to result from the additional resistance to the diffusion of isopentane imposed by the PDMS matrix. Muzzalupo et al. reported activation energy values of 10.1 and 15.4 kJ/mol for the diffusion of hexane and heptane through a PDMS matrix using pulsed field gradient-NMR [15]. Isopentane was presumed to have similar polarity and solubility as hexane and heptane, so the activation energy for isopentane diffusion through PDMS measured by TGA was estimated to be approximately 121–141 kJ/mol. Later, this activation energy was compared with the MWS relaxation of the PAN copolymer since the diffusion process of isopentane occured in conjunction with the molecular motions of the PAN copolymer in the microcapsule shell.

3.2. Dielectric analysis

When the PDMS control sample was analyzed under identical conditions as Film-A, the magnitude of the dielectric loss was less than 2% of the dielectric loss permittivity of Film-A and thus simply was part of the baseline in the experiments on the composite sample. PDMS (α-relaxation at around −123 °C at 1 Hz) [19] and isopentane (bp = 28 °C) [22] generate no significant dielectric response under the test frequencies employed. The temperature and frequency dependence of the dielectric loss permittivity ε'' for Film-A are shown for the first heat (a) and the second heat (b) in Fig. 5. It should be noted that dc conductivity was not significant up to 187 °C. Fig. 6 shows the temperature dependence of the storage permittivity (ε') and $\tan\theta$ together with the loss (ε'') permittivity of Film-A for (a) the first heat and (b) the second heat. Based on the reported T_g values for polyacrylonitrile (80–105 °C) [19] and poly(methacrylonitrile) (67–120 °C) [20], and the content of methacrylonitrile (27 mol%) as determined using NMR spectroscopy, the signal rise in ε' at ca. 100 °C was assigned as the copolymer T_g, i.e. the onset of the softening of

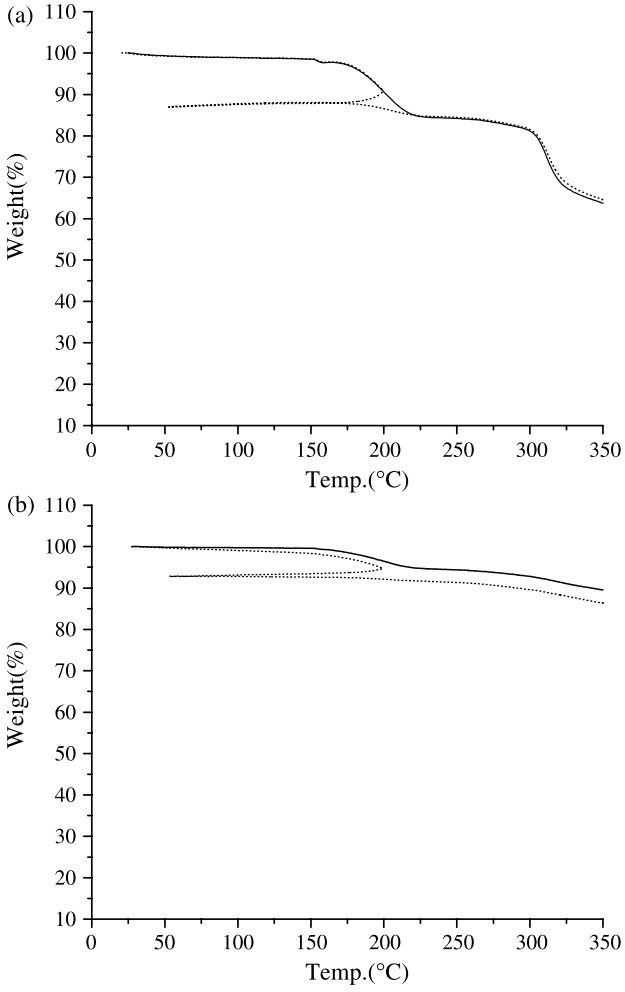

Fig. 3. TGA curves of (a) PAN copolymer microcapsule under cyclic heating (dotted line) and straight heating (solid line); (b) PAN copolymer microcapsule (35 phr) in PDMS under cyclic heating (dotted line) and straight heating (solid line) (5 °C/min heating rate under nitrogen atmosphere).

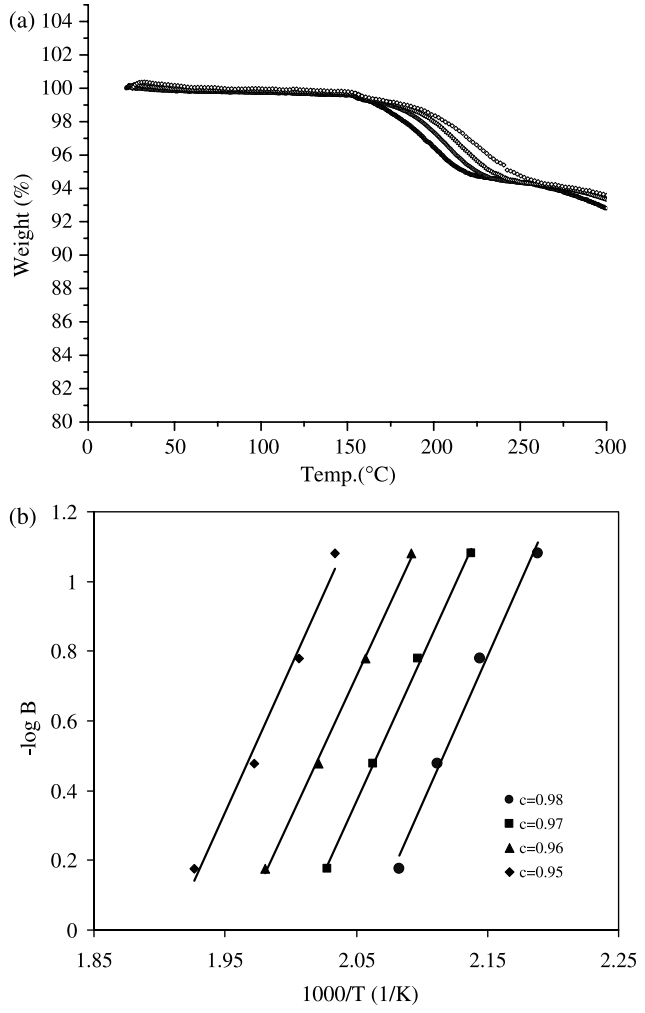

Fig. 4. (a) TGA curves of PAN copolymer microcapsule in PDMS measured at various heating rates. Curves shift from the left to the right (square, circle, triangle and diamond symbols correspond to 5, 10, 20, and 40 °C/min heating rate, respectively, under nitrogen atmosphere); (b) plots of logarithmic heating rate versus reciprocal absolute temperature using the data from (a) for the weight loss process due to the diffusion of isopentane through PAN copolymer shell and PDMS matrix.

the PAN copolymer shell. In the vicinity of T_g, enhanced mobility and/or orientation of the nitrile groups increased ε'. The storage permittivity in the first heat displayed an appreciable decrease after 140 °C that continued until 160 °C followed by a secondary increase up to 200 °C. When the temperature reached 140 °C, the PAN copolymer shell could no longer function as a gas barrier for isopentane. Therefore, the observed decrease of ε' at ca. 140 °C could be attributed to the disruption of the orientation of nitrile groups by the diffusion of isopentane through the shell. In Fig. 4(a), the onset of the weight loss process supports this hypothesis. DEA curves for the second heat cycle (Fig. 6(b)) exhibited trends that are more typical of dielectric dispersions of bulk polymers in that no abnormal reduction in the storage permittivity was observed. For this second heating, now without isopentane, ε' increased gradually from 100 to 200 °C. The major distinguishing characteristics of the second heat curves are summarized as follows: (1) the unusual reduction of ε' was not observed, (2) the magnitude of ε', ε'', and tan δ were all reduced, and (3) the peaks of ε'' and tan δ were broadened. Gupta and Singhal reviewed the effects of heat treatment on polyacrylonitrile films and observed lower values of ε'' and tan δ for heat-treated samples [23]. The change was speculated to be predominantly due to the decrease in the mean square dipole moment of the relaxing segments. Thünemann compared the dielectric relaxation of polyacrylonitrile and a PAN copolymer with methyl acrylate as well as itaconic acid. Samples were examined before and after cyclization induced by heat treatment at 230 °C for 10 h in nitrogen [24]. These researchers reported thermal aging effects, which resulted in reduced relaxation strength, activation energy, and relaxation times. Previous work on the dielectric relaxation studies by Gupta

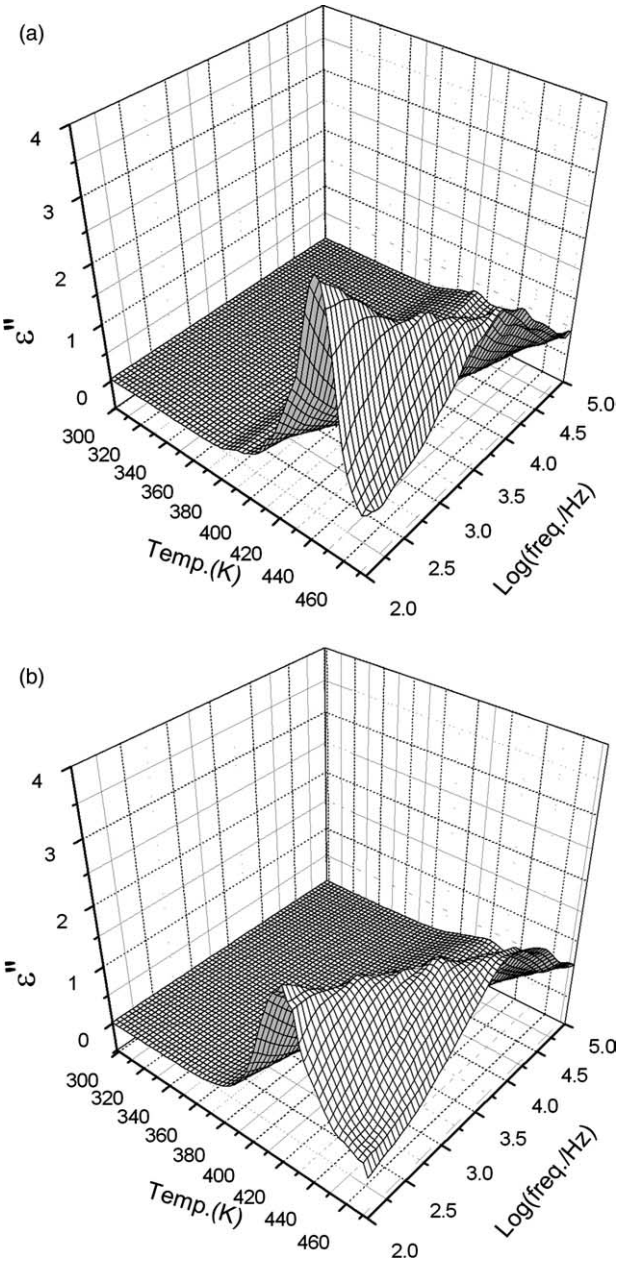

Fig. 5. 3D representation of the frequency and temperature dependence of the dielectric loss permittivity for Film-A (a) first heat (b) second heat.

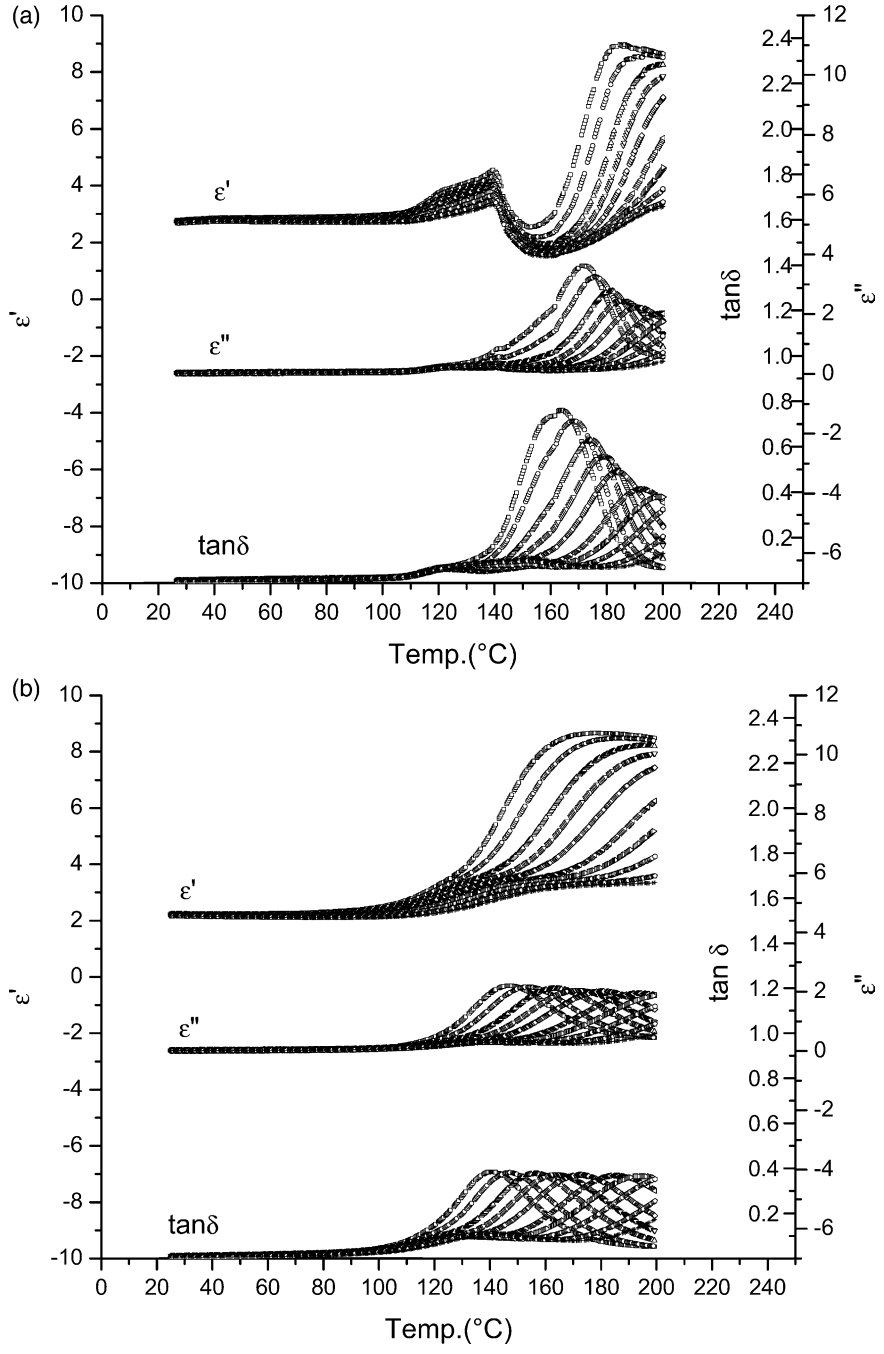

Fig. 6. Temperature dependence of the storage (ε'), tan δ, and loss (ε'') permittivity for Film-A (a) first heat (b) second heat. Symbols for test frequency are (□) 100 Hz, (○) 200 Hz, (△) 500 Hz, (▽) 1 kHz, (◇) 2 kHz, (◁) 5 kHz, (▷) 10 kHz, (⬡) 20 kHz, (⬠) 1 kHz, (+) 1 kHz.

[23], Ishida [25], Saito [26], and Hayakawa [27] used a relatively narrow frequency range from 10^2 to 10^5 Hz, as was also true in our work. The temperature ranges chosen by these workers were limited to below 160 °C (~433 K) due to a rise in dc conductivity (for example, see Fig. 3 in Ref. [28]). On the other hand, Thünemann used a wide frequency range from 10^1 to 10^6 Hz and reported relaxation parameters up to 185 °C (~458 K). The temperature range analyzed in our study was from 180 °C (~453 K) to 198 °C (~471 K), a difficult range to evaluate due to high dc conductivity of polyacrylonitrile as the temperature rises far above T_g. So far, this temperature range has been thought to be responsible for the thermal aging process of nitrile groups [23–27]. Apart from the peak that was related to the α-relaxation process of the microcapsule (ca. 100 °C), the relaxation peaks of our interest were virtually unaffected by the α-process and are well separated from such peaks. In fact, the rising ε'' peaks interpreted as Dc conductivity in the previous studies [23,28] were considered as the onset of the high temperature relaxation process due to MWS interfacial polarization in our experiments.

For quantitative treatment of observed MWS relaxation spectra, the semi empirical function of Havriliak–Negami was

used [29].

$$\varepsilon^*(\omega) = \varepsilon_\infty + \frac{\Delta\varepsilon}{(1 + (i\omega\tau_{HN})^\alpha)^\gamma} \quad (3)$$

where ε_∞ is the limiting high-frequency permittivity, and $\Delta\varepsilon = \varepsilon_{st} - \varepsilon_\infty$ denotes the relaxation strength where ε_{st} is the static dielectric permittivity. The α is a parameter characterizing a symmetrical broadening of relaxation times, while γ characterizes an asymmetrical broadening ($0 < \alpha,\gamma \leq 1$). τ_{HN} represents the characteristic relaxation time. For frequency dependent conductivity contribution, the following exponential function was used [30]

$$\varepsilon''(\omega) = \frac{\sigma_0}{\varepsilon_0 \omega^s} \quad (4)$$

where σ_0 and s are fitting parameters, σ_0 denotes the contribution of mobile charge carriers to the loss permittivity, and ε_0 permittivity of free space. In Fig. 7, the fit of ε'' is shown with experimental values for Film-A. Noticeable changes were in the decreasing values of the relaxation strength and relaxation times in the second heat of the film (Table 1).

Using a similar experimental approach for Film-A, the PAN copolymer microcapsules (30 phr) in PDMS (Film-B) were prepared separately and analyzed over five successive thermal cycles and the model fitting results are listed in Table 2. Relaxation times as well as relaxation strength decreased significantly in the second heat in a similar fashion to results for Film-A. The effect of thermal cycling after the second heating was minimal. The relaxation strengths over successive thermal cycling are illustrated in Fig. 8 using the data from Table 2. In the first heat, the relaxation strength decreased with increasing temperature; whereas, it only slightly increased in subsequent heating cycles. The relaxation times, τ_{HN}, arising from the Havriliak–Negami model (Table 2) were fitted to the Arrhenius equation to determine an activation energy according to

$$\tau = \tau_0 \exp\left(\frac{E_a}{RT}\right) \quad (5)$$

where τ_0 is the limiting relaxation time at infinite temperature, E_a and R are the apparent activation energy and the gas constant, respectively (Fig. 9). All the data presented in Fig. 9 are seen to be well represented by Eq. (5) and the E_a values were obtained from the slopes. The activation energy values decreased over successive thermal cycling (Table 3). Unusually high activation energy, compared to the results from the rest of the thermal cycles, was obtained on the first film heating. One possible explanation is that the relaxation process occurring in the first heat was influenced by the diffusion of isopentane molecules. Also, it is interesting to recall that the TGA analysis yielded an activation energy of the diffusion of isopentane through the PAN copolymer of 121 kJ/mol for the microcapsule and 131 kJ/mol for Film-A (slight isopentane concentration differences existed for TGA and DEA). Such E_a value agreement suggested an identical relaxation process.

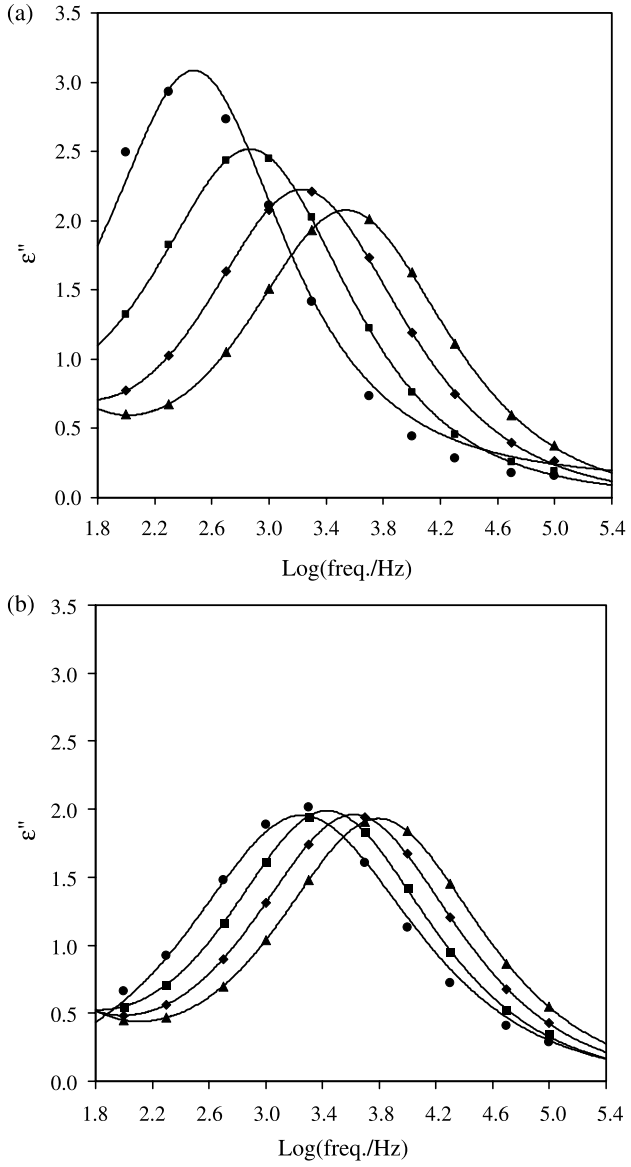

Fig. 7. Experimental values of the loss permittivity of the Film-A (a) the first heat (b) the second heat; (circle, square, diamond, and triangle corresponds to 453.2, 459.2, 465.2, and 471.2 K, respectively) and fits of the Havriliak–Negami and conductivity contribution according to Eqs. (1) and (2). The fit parameters are listed in Table 1.

The diffusion process of the isopentane seemed to be virtually complete after the first heat, which reinforced the TGA results. It was also observed that successive thermal cycles affected the PAN copolymer embedded in the PDMS matrix as revealed by the progressive decrease in activation energy.

The effect of the concentration of the PAN copolymer microcapsule was investigated by analyzing relaxation data of samples with various concentrations of microcapsules in the PDMS matrix under otherwise identical experimental conditions. Tables 4 and 5 present a summary of the relaxation parameters obtained from this concentration variation. Activation energies were evaluated from the data in Tables 4 and 5 in the same manner used for Film-B and the results are summarized in Table 6.

Table 1
Havriliak–Negami parameters of Film-A (PAN copolymer microcapsules in PDMS matrix (35 phr)) for the 1st and 2nd heating

Cycle	Temp. (K)	τ_{HN} (s)	α	γ	$\Delta\varepsilon$	σ_0 $((\Omega\,m)^{-1})$	s
1st	453.2	5.562×10^{-4}	0.901	0.928	6.479	–	–
	459.2	2.079×10^{-4}	0.817	0.995	6.230	1.87×10^{-11}	0.28
	465.2	9.685×10^{-5}	0.808	0.951	6.088	2.33×10^{-10}	0.73
	471.2	4.551×10^{-5}	0.795	0.998	5.732	6.49×10^{-10}	0.86
2nd	453.2	9.416×10^{-5}	0.742	0.952	6.013	–	–
	459.2	6.216×10^{-5}	0.793	0.941	5.640	3.02×10^{-11}	0.81
	465.2	3.853×10^{-5}	0.782	0.986	5.569	7.50×10^{-10}	0.93
	471.2	2.532×10^{-5}	0.782	0.999	5.462	6.86×10^{-10}	0.89

Table 2
Havriliak–Negami parameters of Film-B (PAN copolymer microcapsules in PDMS matrix (30 phr)) over five successive thermal cycling

Cycle	Temp. (K)	τ_{HN} (s)	α	γ	$\Delta\varepsilon$	σ_0 $((\Omega\,m)^{-1})$	s
1st	453.2	4.183×10^{-4}	0.841	0.988	4.445	4.42×10^{-11}	0.36
	457.2	2.187×10^{-4}	0.838	0.987	4.169	2.83×10^{-11}	0.31
	461.2	1.177×10^{-4}	0.830	0.997	3.915	1.82×10^{-11}	0.27
	467.2	5.177×10^{-5}	0.811	0.954	3.917	1.12×10^{-10}	0.57
	471.2	2.995×10^{-5}	0.801	0.985	3.705	1.21×10^{-10}	0.57
2nd	453.2	4.728×10^{-5}	0.861	0.845	3.283	1.37×10^{-11}	0.27
	457.2	3.387×10^{-5}	0.828	0.880	3.534	6.23×10^{-11}	0.51
	461.2	2.393×10^{-5}	0.813	0.927	3.543	1.09×10^{-10}	0.59
	467.2	1.436×10^{-5}	0.796	0.988	3.500	1.80×10^{-10}	0.65
	471.2	1.070×10^{-5}	0.797	0.996	3.429	1.44×10^{-10}	0.61
3rd	453.2	3.621×10^{-5}	0.849	0.877	3.137	–	–
	457.2	2.694×10^{-5}	0.824	0.900	3.347	2.83×10^{-11}	0.44
	461.2	1.968×10^{-5}	0.811	0.939	3.357	4.86×10^{-11}	0.51
	467.2	1.256×10^{-5}	0.796	0.995	3.338	8.46×10^{-11}	0.59
	471.2	9.859×10^{-6}	0.798	0.996	3.295	6.79×10^{-11}	0.55
4th	453.2	3.811×10^{-5}	0.841	0.932	3.012	–	–
	457.2	3.015×10^{-5}	0.830	0.896	3.230	1.22×10^{-11}	0.34
	461.2	2.233×10^{-5}	0.817	0.925	3.260	2.42×10^{-11}	0.44
	467.2	1.451×10^{-5}	0.803	0.972	3.252	4.88×10^{-11}	0.54
	471.2	1.115×10^{-5}	0.798	0.993	3.223	5.72×10^{-11}	0.56
5th	453.2	4.449×10^{-5}	0.833	0.954	3.050	–	–
	457.2	3.605×10^{-5}	0.835	0.891	3.194	–	–
	461.2	2.725×10^{-5}	0.821	0.905	3.292	1.75×10^{-11}	0.41
	467.2	1.781×10^{-5}	0.808	0.940	3.284	3.93×10^{-11}	0.53
	471.2	1.379×10^{-5}	0.803	0.958	3.263	5.48×10^{-11}	0.57

Although the statistical agreement was less satisfactory for these results than for Film-B, the values were deemed acceptable for further analysis. It was concluded that the activation energy of the first heat was consistently higher than that of the second heat. It should be noted that the average activation energy of the second heat (120 ± 12 kJ/mol) was comparable to the corresponding result from TGA analysis (131 ± 14 kJ/mol) in this report. These results also match-up well with those of Thünemann who used a PAN copolymer with 2–6 mol% acrylate and itaconic acid (139 ± 1 kJ/mol) [24]. The activation energy obtained from this study did not vary significantly with the concentration of the microcapsules in the samples. This finding was important since it implies that the PDMS matrix did not affect the observed relaxation mechanism of the PAN copolymer significantly and the MWS relaxation behavior as observed in this study was primarily reflecting the dispersion behavior of the PAN copolymer shell.

The relaxation strength data of the PAN copolymer in the PDMS matrix provided in Tables 4 and 5 are plotted in Fig. 10 to indicate temperature dependence and in Fig. 11 to show concentration dependence, respectively. From Fig. 10, the relaxation strength during the first heat for all concentrations is seen to generally decrease; whereas, the second heat produced a slightly increasing trend. When the relaxation strength was replotted as a function of the concentration (Fig. 11), the first heat data (hollow symbols) were scattered, however, showed overall increasing trends with increasing concentration. The relaxation strength of the second heat (filled symbols), after most isopentane diffused out of the system, showed less scatter and an increase in magnitude with increasing concentration. A previous dielectric study on a PAN copolymer using bulk films prepared from a solution cast process reported relaxation strength values ranging from 30 to 70 for a PAN and PAN copolymer [24]. Our results (less than 7 at the 35 phr level)

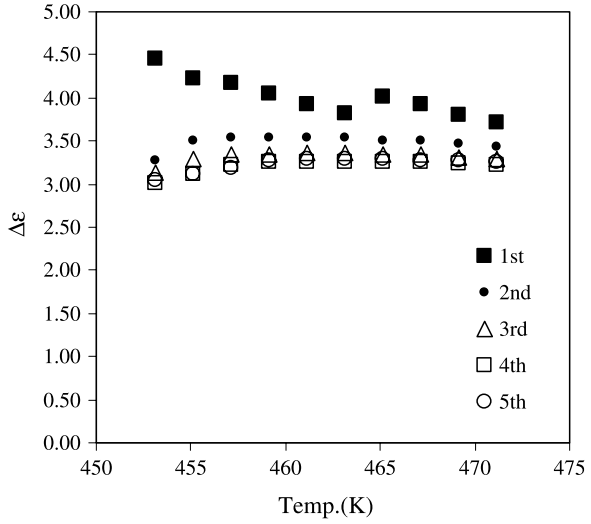

Fig. 8. Temperature dependence of the relaxation strength of Film-B (PAN copolymer microcapsule in PDMS matrix (30 phr) over five successive thermal cycling.

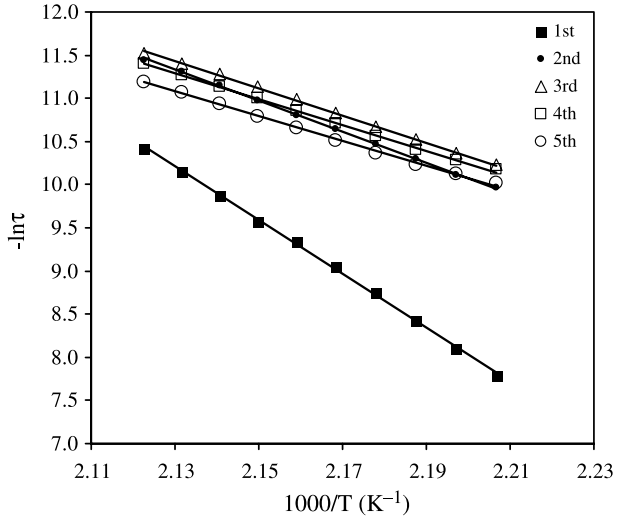

Fig. 9. Arrhenius plot for the determination of the activation energy of the dielectric relaxation over multiple thermal cycling for Film-B (PAN copolymer microcapsule in PDMS matrix (30 phr)).

Table 3
Values of activation energies over successive thermal cycling

Cycle	E_a (kJ/mol)	r^2
1st	258	0.999
2nd	149	0.999
3rd	131	0.998
4th	124	0.999
5th	119	0.998

suggest that increasing the concentration of the microcapsules would lead to a similarly high relaxation strength. The magnitude of the relaxation strength encountered in previous investigations is postulated as the limiting case of our present study. The trends of our experimental results follow the simple theory due to Sillars that explains the MWS relaxation strength of heterogeneous system composed of a small volume fraction of inclusions distributed in an insulating matrix as follows [31]

$$\Delta\varepsilon = \frac{\phi}{A}\varepsilon_m \tag{6}$$

where ϕ, A, and ε_m represents the volume fraction of the conducting inclusions, the polarization factor along the axis of the applied electric field (1/3 for random orientation), and the permittivity of the matrix, respectively.

The Havriliak–Negami parameters α and γ of the MWS relaxation obtained from our experiments were approximately 0.8 and close to 1, respectively, for most of the samples as we varied microcapsule concentrations and multiple thermal cyclings. These results are also consistent with those of Thünemann who reported that the value of α was 0.2 at 27 °C, and increased to 0.8 at 187 °C, and further predicted it to be 1 (perfect Debye behavior) at 217 °C for a polyacrylonitrile neat film (with fixed value of $\gamma = 1$). He also pointed out that the Debye-like relaxation behavior of polyacrylonitrile could result for two cases: (1) the inter- and intra-molecular interactions for all dipoles are identical, and (2) the movements within the surroundings of the relaxing objects are much faster than the relaxation itself (motional averaging) [32]. In our studies, since the PDMS relaxes faster than PAN copolymer at the surface of the microcapsules, the effect of motional averaging might have contributed to the quasi-Debye relaxation behavior we observed.

The level of deviation from the single relaxation time model in time domain was evaluated using the Kohlrausch–Williams–Watts (KWW) function:

$$\Phi(t) = \exp\left[-\left(\frac{t}{\tau_{KWW}}\right)^{\beta}\right] \tag{7}$$

where the $\beta(0 < \beta \leq 1)$ parameter describes the nonexponential character of the relaxation function, and the τ_{KWW} is the KWW relaxation time. According to the formalism of Alvarez et al., the Havriliak–Negami parameters α and γ were reduced to a single parameter of the stretched exponential β as follows [13,33].

$$\beta = (\alpha\gamma)^{1/1.23} \tag{8}$$

In Fig. 12, values of the parameter β evaluated from the data in Tables 2, 4, and 5 using Eq. (8) are plotted. In Fig. 12(a), the β for the first heat (filled square) was slightly larger than the β of the second and subsequent heats between 450 and 460 K. All values of β were found to be centered around 0.8. Similar results were obtained when β was evaluated as a function of the concentration of microcapsules (Fig. 12(b)). Although data scatter was present, it was found that β was smaller for the second heat (filled symbols). Our experimental results $\beta \sim 0.8$ obtained within the chosen analytical window was much higher than most reported values of β for an α-relaxation range from 0.39 to 0.68 [30,34]. The relaxation events we monitored appeared to be thermally activated since the β increased slightly from approximately 0.78 to 0.82 (in the direction toward a single Debye system) as the temperature was

Table 4
Havriliak–Negami parameters of PAN copolymer microcapsules in PDMS matrix (1st heat)

phr	Temp. (K)	τ_{HN} (s)	α	γ	$\Delta\varepsilon$	σ_0 ($(\Omega\,m)^{-1}$)	s
5	453.2	2.128×10^{-4}	0.894	0.973	0.290	–	–
	457.2	1.371×10^{-4}	0.889	0.962	0.258	–	–
	461.2	8.189×10^{-5}	0.889	0.989	0.213	–	–
	467.2	5.551×10^{-5}	0.906	0.760	0.212	1.49×10^{-11}	0.62
	471.2	3.551×10^{-5}	0.888	0.812	0.194	3.68×10^{-11}	0.74
10	453.2	2.854×10^{-4}	0.824	0.996	0.958	–	–
	457.2	1.780×10^{-4}	0.827	0.961	0.837	–	–
	461.2	9.745×10^{-5}	0.857	0.992	0.625	–	–
	467.2	5.100×10^{-5}	0.896	0.892	0.480	–	–
	471.2	3.807×10^{-5}	0.874	0.804	0.516	1.42×10^{-11}	0.56
20	453.2	4.236×10^{-4}	0.802	0.970	3.552	–	–
	457.2	2.225×10^{-4}	0.810	0.985	2.854	–	–
	461.2	1.202×10^{-4}	0.839	0.984	2.189	–	–
	467.2	5.772×10^{-5}	0.878	0.926	1.672	–	–
	471.2	4.201×10^{-5}	0.862	0.849	1.760	8.08×10^{-11}	0.71
35	453.2	5.562×10^{-4}	0.901	0.928	6.479	–	–
	457.2	3.327×10^{-4}	0.867	0.908	6.222	–	–
	461.2	1.166×10^{-4}	0.817	0.993	5.801	2.42×10^{-11}	0.44
	467.2	7.269×10^{-5}	0.795	0.983	6.047	4.88×10^{-9}	0.54
	471.2	4.551×10^{-5}	0.795	0.998	5.732	5.72×10^{-10}	0.56

Table 5
Havriliak–Negami parameters of PAN copolymer microcapsules in PDMS matrix (2nd heat)

phr	Temp. (K)	τ_{HN} (s)	α	γ	$\Delta\varepsilon$	σ_0 ($(\Omega\,m)^{-1}$)	s
5	453.2	7.041×10^{-5}	0.966	0.833	0.127	–	–
	457.2	7.016×10^{-5}	0.999	0.590	0.161	–	–
	461.2	4.958×10^{-5}	0.932	0.653	0.181	–	–
	467.2	2.902×10^{-5}	0.886	0.748	0.184	2.33×10^{-11}	0.71
	471.2	2.000×10^{-5}	0.861	0.819	0.184	3.53×10^{-11}	0.76
10	453.2	6.404×10^{-5}	0.882	0.996	0.356	–	–
	457.2	5.467×10^{-5}	0.915	0.853	0.368	–	–
	461.2	4.762×10^{-5}	0.924	0.713	0.420	–	–
	467.2	2.902×10^{-5}	0.870	0.779	0.464	–	–
	471.2	2.067×10^{-5}	0.854	0.829	0.464	1.49×10^{-11}	0.56
20	453.2	7.431×10^{-5}	0.863	0.993	1.378	–	–
	457.2	5.690×10^{-5}	0.874	0.955	1.376	–	–
	461.2	4.751×10^{-5}	0.893	0.849	1.421	–	–
	467.2	3.235×10^{-5}	0.863	0.820	1.615	2.80×10^{-11}	0.58
	471.2	2.340×10^{-5}	0.850	0.856	1.605	8.08×10^{-11}	0.66
35	453.2	9.416×10^{-5}	0.742	0.952	6.013	–	–
	457.2	7.416×10^{-5}	0.809	0.904	5.534	4.33×10^{-11}	0.50
	461.2	5.252×10^{-5}	0.787	0.960	5.621	3.49×10^{-11}	0.88
	467.2	3.313×10^{-5}	0.780	0.996	5.537	8.64×10^{-10}	0.94
	471.2	2.532×10^{-5}	0.782	0.999	5.462	6.86×10^{-10}	0.89

increased. This was true for most of the thermal cycling results except from the first heat (that incorporated the influence of the diffusion of isopentane) as shown in Fig. 12(a). Therefore, our result of $\beta\sim0.8$ suggests a thermally activated molecular motion of the nitrile groups not consumed in an intra-molecular cyclization process, phenomena already demonstrated to occur in the temperature range we investigated by previous spectroscopic experiments [6,18]. The mechanism of cyclization of polyacrylonitrile is random initiation by hydrogens α to the nitrile [6]. The presence of polymethacrylonitrile, which does

Table 6
Activation energies with varying concentrations of microcapsules in PDMS matrix

Concentration (phr)	1st heat		2nd heat	
	E_a (kJ/mol)	r^2	E_a (kJ/mol)	r^2
5	172	0.988	130	0.942
10	208	0.980	111	0.958
20	229	0.986	109	0.981
35	254	0.972	130	0.995

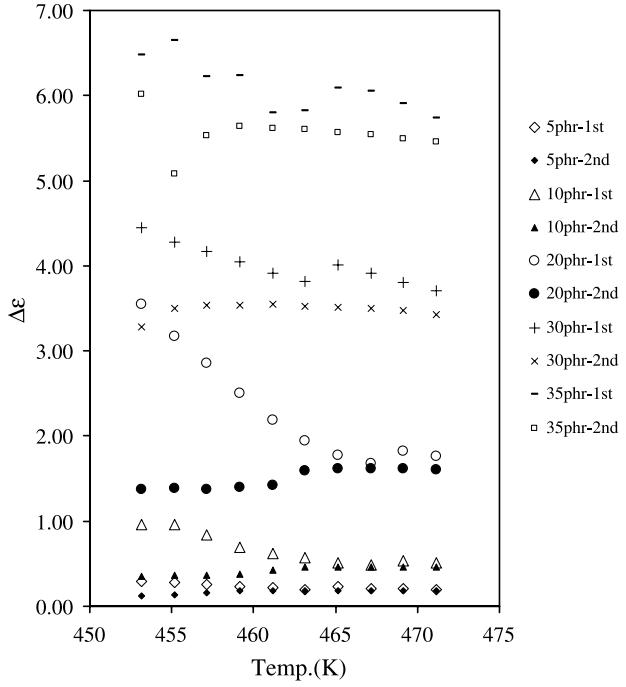

Fig. 10. Temperature dependence of the relaxation strength of PAN copolymer microcapsule in PDMS matrix.

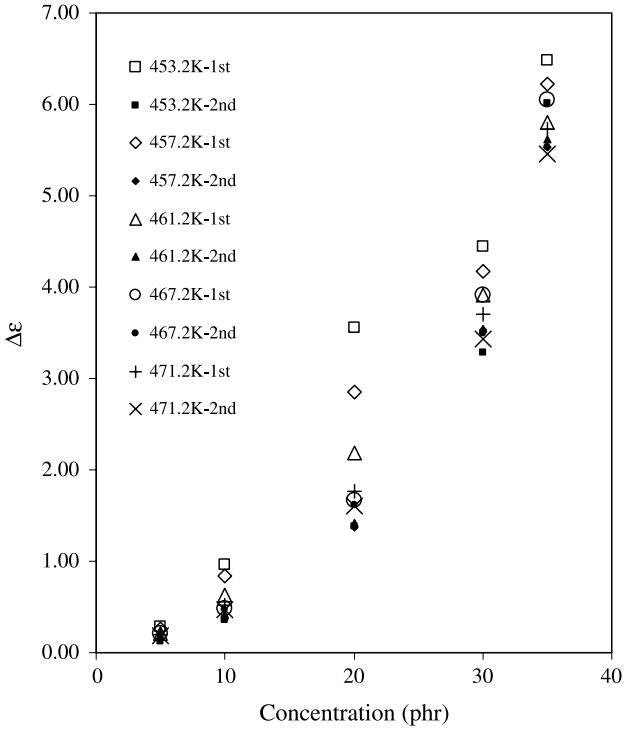

Fig. 11. Concentration dependence of the relaxation strength of PAN copolymer microcapsule in PDMS matrix.

not contain such hydrogens, in the PAN copolymer (as in our study), is expected to reduce the tendency for cyclization. Thus, if pure PAN microcapsules were dispersed in the PDMS matrix, the relaxation mechanism identified in this work would probably have yielded results much similar to previous studies.

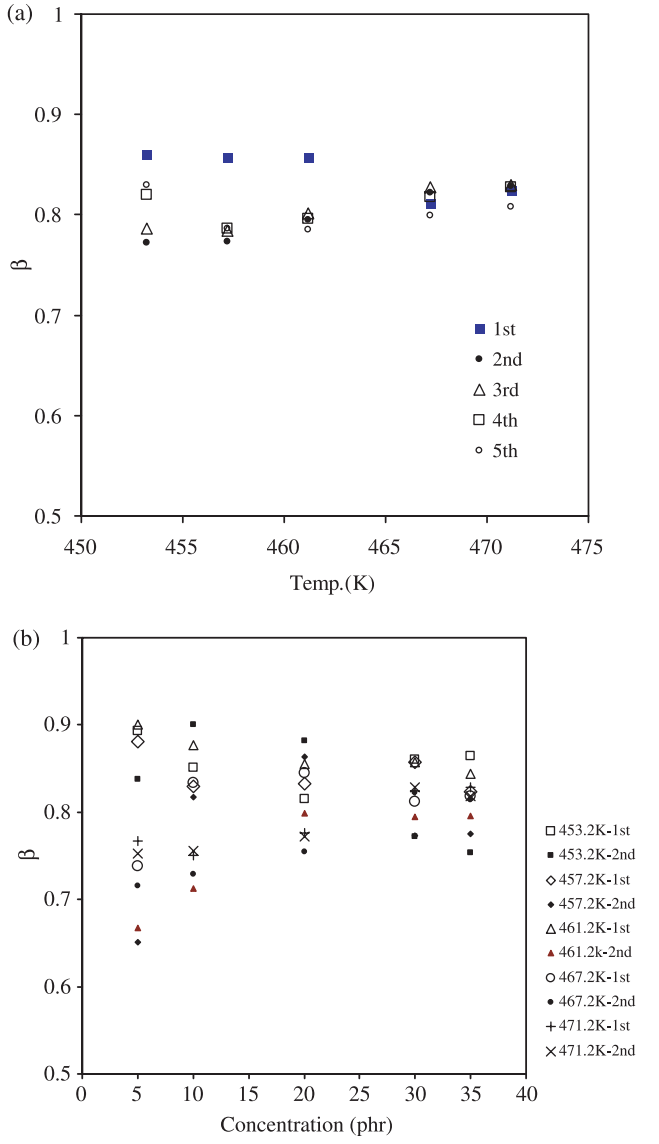

Fig. 12. (a) Temperature dependence of β in KWW over successive thermal cycling (b) concentration dependence of β in KWW relaxation function.

4. Summary

Dielectric analysis performed on a PAN copolymer microcapsule dispersed in a PDMS matrix exhibited a MWS interfacial polarization in the temperature range where analysis was difficult due to high dielectric loss due to the thermal aging of the neat PAN or PAN copolymer films. The Arrhenius activation energies, Havriliak–Negami, and KWW parameters obtained in this study were found to be close to the extension of the previous studies performed at lower temperature. The influence of PDMS matrix on various relaxation parameters was found to be minimal. The experimental results suggested that by proper choice of matrix material and experimental conditions, MWS relaxation behavior of the total composite system could be used to study the relaxation behavior of the dispersed phases (especially true when the relaxation of interest is well separated from that of PDMS).

Acknowledgements

Authors would like to thank Sovereign Specialty Chemicals for supplying the PAN copolymer microcapsules. This work was supported by DARPA/DSO and NASA Langley Research Center, grant numbers NAG-1-03026 and NAG-1-03052. The program managers for this work are Dr John Main (DARPA/DSO) and Dr Garnett Horner (NASA). The authors gratefully acknowledge their financial support.

References

[1] Ikada E, Watanabe T. J Polym Sci 1972;10:3457.
[2] Kenyon AS, Rayford McCJ. J Appl Polym Sci 1979;23:717.
[3] Cook M, Williams G, Jones TT. Polymer 1975;16:835.
[4] Kowalewski T, Tsarevsky NV, Matyjaszewski K. J Am Chem Soc 2002; 124:10632.
[5] Ogura K, Kawamura S, Sobue H. Macromolecules 1971;4:79.
[6] Xue TJ, McKinney MA, Wilkie CA. Polym Degrad Stab 1997;58:193.
[7] Perrier G, Bergeret A. J Appl Phys 1995;77:2651.
[8] Chung KT, Sabo A, Pica P. J Appl Phys 1982;53:6867.
[9] Boersma A, Wubbenhorst M, Turnhout J. Macromolecules 1997;30:2915.
[10] Hayward D, Pethrick RA, Siriwittayakorn T. Macromolecules 1992;25: 1480.
[11] Zhang HZ, Serkine K, Hanai T, Koizumi N. Colloid Polym Sci 1983;261: 381.
[12] Asami K. Prog Polym Sci 2002;27:1617.
[13] Alvarez F, Alegria A, Colmenero J. Phys Rev B 1991;44:7306.
[14] Park, T, Lizotte JR, Cromer F, Long, TE. Private Communication.
[15] Muzzalupo R, Ranieri GA, Golemme G, Drioli E. J Appl Polym Sci 1999; 74:1119.
[16] Minagawa M, Takasu T, Shinozaki S, Yoshii F, Morishita N. Polymer 1995;36:2343.
[17] Inoue Y, Koyama K, Chujo R, Nishioka A. Polym Lett 1973;11:55.
[18] Grassie N, McNeill IC. Eur Polym J 1972;8:243.
[19] Van Krevelen DW. Properties of polymers. New York: Elsevier; 1976.
[20] Katircioglu TY, Guven O. J Appl Polym Sci 2001;82:1936.
[21] Flynn HJ, Wall LA. Polym Lett 1966;4:329.
[22] Reid RC, Prausnitz JM, Sherwood TK. The properties of gases and liquids. 3rd ed. New York: McGraw-Hill; 1977.
[23] Gupta AK, Singhal RP. J Appl Polym Sci 1982;27:4101.
[24] Thünemann AF. Macromolecules 2000;33:1790.
[25] Ishida Y, Amano O, Takayanagi M. Kolloid Z 1960;172:129.
[26] Saito S, Nakajima T. J Appl Polym Sci 1953;2:93.
[27] Hayakawa R, Nishi T, Arisawa K, Wada Y. J Polym Sci A-2 1967;5:165.
[28] Gupta AK, Chand N. J Polym Sci, Polym Phys 1980;18:1125.
[29] Havriliak S, Negami S. Polymer 1967;8:101.
[30] Boese D, Kremer F. Macromolecules 1990;23:829.
[31] Sillars RWJ. Inst Electr Eng 1937;80:378.
[32] Spiess HW. Adv Polym Sci 1985;66:23.
[33] Alegria A, Echevarria E, Goiyiandia L, Telleria I, Colmenero J. Macromolecules 1995;28:1516.
[34] Cendoya I, Alegria A, Alberdi JM, Colmenero J, Grimm H, Richer D, et al. Macromolecules 1999;32:4065.